




## Article

# Cleanup and Conversion of Biomass Liquefaction Aqueous Phase to C<sub>3</sub>–C<sub>5</sub> Olefins over Zn<sub>x</sub>Zr<sub>y</sub>O<sub>z</sub> Catalyst

Stephen D. Davidson <sup>1</sup>, Juan A. Lopez-Ruiz <sup>1</sup>, Matthew Flake <sup>1</sup>, Alan R. Cooper <sup>1</sup>, Yaseen Elkasabi <sup>2</sup>, Marco Tomasi Morgano <sup>3</sup>, Vanessa Lebarbier Dagle <sup>1</sup>, Karl O. Albrecht <sup>4</sup> and Robert A. Dagle <sup>1,\*</sup>

<sup>1</sup> Energy and Environment Directorate, Institute for Integrated Catalysis Pacific Northwest National Laboratory, Richland, WA 99352, USA; stephen.davidson@pnnl.gov (S.D.D.); juan.lopezruiz@pnnl.gov (J.A.L.-R.); Matthew.Flake@pnnl.gov (M.F.); Alan.Cooper@pnnl.gov (A.R.C.); vanessa.dagle@pnnl.gov (V.L.D.)

<sup>2</sup> USDA-ARS Eastern Regional Research Center, Wyndmoor, PA 19038, USA; yaseen.elkasabi@usda.gov

<sup>3</sup> ARCUS Greencycling Technologies GmbH, 71638 Ludwigsburg, Germany; Marco.TomasiMorgano@arcus-greencycling.technology

<sup>4</sup> Archer Daniels Midland Company, James R. Randall Research Center, Decatur, IL 62521, USA; Karl.Albrecht@adm.com

\* Correspondence: robert.dagle@pnnl.gov; Tel.: +1-(509)-371-6264

Received: 14 October 2019; Accepted: 1 November 2019; Published: 6 November 2019



**Abstract:** The viability of using a Zn<sub>x</sub>Zr<sub>y</sub>O<sub>z</sub> mixed oxide catalyst for the direct production of C<sub>4</sub> olefins from the aqueous phase derived from three different bio-oils was explored. The aqueous phases derived from (i) hydrothermal liquefaction of corn stover, (ii) fluidized bed fast pyrolysis of horse litter, and (iii) screw pyrolysis of wood pellets were evaluated as feedstocks. While exact compositions vary, the primary constituents for each feedstock are acetic acid and propionic acid. Continuous processing, based on liquid–liquid extraction, for the cleanup of the inorganic contaminants contained in the aqueous phase was also demonstrated. Complete conversion of the carboxylic acids was achieved over Zn<sub>x</sub>Zr<sub>y</sub>O<sub>z</sub> catalyst for all the feedstocks investigated. The main reaction products from each of the feedstocks include isobutene (>30% selectivity) and CO<sub>2</sub> (>23% selectivity). Activity loss from coking was also observed, thereby rendering deactivation of the Zn<sub>x</sub>Zr<sub>y</sub>O<sub>z</sub> catalyst, however, complete recovery of catalyst activity was observed following regeneration. Finally, the presence of H<sub>2</sub> in the feed was found to facilitate hydrogenation of intermediate acetone, thereby increasing propene production and, consequently, decreasing isobutene production.

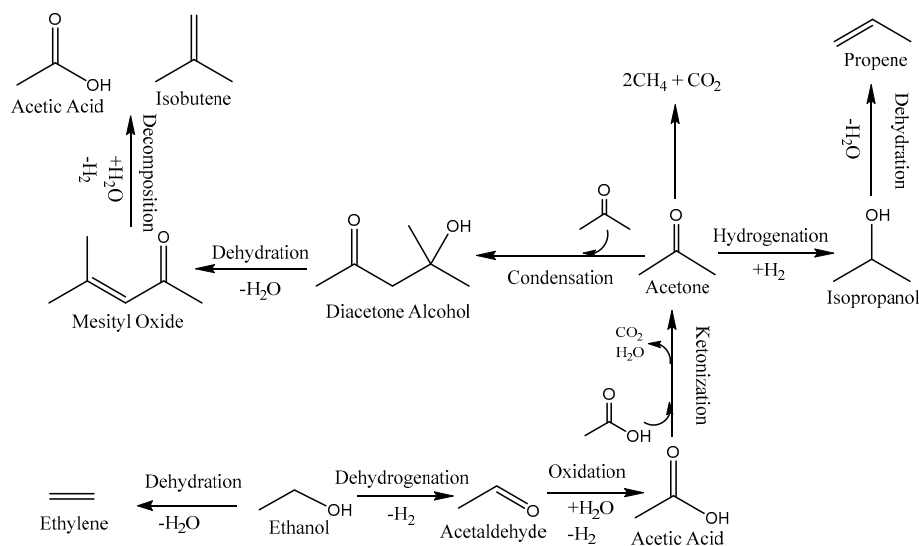
**Keywords:** biomass-derived aqueous phase upgrading; olefin production; oxide catalyst zinc–zirconia

## 1. Introduction

Biomass has received much attention as a renewable source for both fuels and chemicals. While there are a wide range of approaches for biomass conversions, a commonality is high cost of processing leading to a high minimum fuel selling price [1–4]. Direct liquefaction of biomass is an appealing approach as much of the hydrocarbon structure can be preserved [5–7]. Processes with direct liquefaction include hydrothermal liquefaction (HTL) and different permutations of pyrolysis that includes fast pyrolysis (FP), catalytic fast pyrolysis (CFP), and intermediate screw pyrolysis (SP) [8–11]. Regardless of approach, aqueous and organic phases can be segregated by gravity separation. While the organic phase has a lower oxygen content, and consists of molecules typically more suited for fuel, the aqueous phase typically comprises a mixture of light oxygenates that are difficult to separate [1,12].

Thus, the aqueous phase is usually considered a waste stream. Several recent works have reported how the aqueous phase can be converted to different co-products, in order to improve the overall carbon efficiency of the liquefaction process [4,12,13]. For example, we recently reported the co-production of either H<sub>2</sub> or propene, from the aqueous phase, and the resulting process economics for producing fuel from the organic phase [13]. From this work, it was found that the largest impact on minimum fuel selling price is increasing the utilization of carbon from the biomass, including as the sale of co-products [13].

With one pathway to co-products utilizing the aqueous phase from biomass liquefaction already demonstrated, the next step is to expand the platform of potential product compounds to make the biorefinery more versatile. Olefins are a promising group of co-products to produce with isobutene being particularly valuable as it is easily converted to fuel additives, solvents, and butyl rubber products [14–18]. Recently, Zn<sub>x</sub>Zr<sub>y</sub>O<sub>z</sub> catalysts have been identified as having a unique combination of surface acidic and basic sites, generating a cascade reaction network (Scheme 1) [19–22]. This cascade network allows for the direct conversion of ethanol to isobutene in a single reactor bed [15,22]. Ethanol first undergoes ethanol dehydrogenation and ketonization reactions thus producing acetone. ZnO addition offers the necessary basic sites while also suppressing most of the strong acid sites responsible for undesirable ethanol dehydration. Acetone then undergoes aldol condensation and C–C cleavage over acid sites, while the formation of acetone decomposition products (CH<sub>4</sub> and CO<sub>2</sub>) is largely suppressed [22]. Recently, a complete loop starting from syngas and ending with isobutene oligomerization to jet fuel was also demonstrated [15]. In addition, it has been demonstrated that the Zn<sub>x</sub>Zr<sub>y</sub>O<sub>z</sub> catalyst is able to convert larger alcohols, and also carboxylic acids and ketones, into mixed olefin streams [22–24]. As previously demonstrated, the reaction mechanism involves the conversion of alcohols into carboxylic acids before undergoing subsequent reaction steps [22]. This makes the Zn<sub>x</sub>Zr<sub>y</sub>O<sub>z</sub> catalyst promising for the direct conversion of carboxylic acids present in the aqueous phase from biomass liquefaction to olefin products.



**Scheme 1.** Reaction network of ethanol to isobutene and major side products adapted from Smith et al. [22].

In this work we examine the feasibility of directly using biomass liquefaction-derived aqueous phases for the direct production of olefins. Three different aqueous phases are studied, derived from hydrothermal liquefaction (supplied by PNNL, PNNL-HTL), a modular fast pyrolysis (supplied by USDA-ARS, USDA-FP), and a screw pyrolysis (supplied by KIT, KIT-SP). The Zn<sub>x</sub>Zr<sub>y</sub>O<sub>z</sub> catalyst (specific composition Zn<sub>1</sub>Zr<sub>2.5</sub>O) was used for the direct production of C<sub>4</sub>+ olefins. Finally, the effect

of a gas environment was also investigated to study the effects on product selectivity with a model feedstock of ethanol.

## 2. Results and Discussion

### 2.1. Feedstock Cleanup with Continuous Liquid–Liquid Extraction

In our prior work, a batch process was used to separate the target organics (carboxylic acids and alcohols) from the carbon treated stream [13]. The process worked well for high concentrations (~30 wt %) of carboxylic acids, however, we developed a continuous liquid–liquid extraction (LLE) (Figure 1) system to process the aqueous streams with lower concentrations of organics.

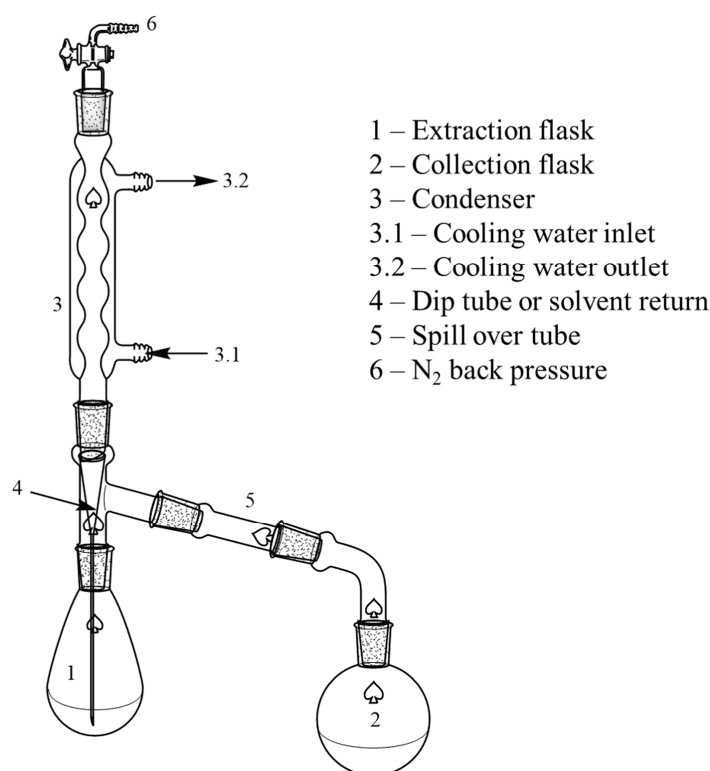


**Figure 1.** Continuous liquid–liquid extraction apparatus. Operation details can be found in Appendix A.

Details on the preparation of the PNNL-HTL feedstock were previously reported [13]. As received, the feedstocks had a different total organic concentration (based on LC composition), 26.2 wt % for KIT-SP, 14.6 wt % for USDA-FP, and 32.6 wt % for PNNL-HTL. For all feedstocks, acetic acid was the most abundant compound. The composition of the different feedstocks is summarized in Table 1. The full analysis can be found in the Supporting Information. A carbon treatment was performed first to remove color bodies and other compounds from the as received samples as it has been reported to cause deactivation during catalytic upgrading [13]. Following carbon treatment, the organic concentration decreased <10% due to adsorption onto the carbon surface, however, we also observed a loss of aqueous phase as it was retained in the porous structure of the carbon. The overall aqueous loss depended on the number of carbon treatments required for each sample. For example, the USDA-FP feedstock required two rounds of carbon treatment and lost 26.8% of the mass, while the KIT-SP feedstock required five rounds of carbon treatment and lost 69.6% of the mass (~13.6% during each carbon treatment). As previously shown, the carbon treatment removed all the color bodies from the sample and the feedstocks became water clear (see Supporting Figure S1) [13]. However, the carbon treatment increased the inorganic concentration of the feedstock, particularly for K, Mg, Na, and P from ≤100 ppm in all cases to as high as 1560 ppm K in USDA-FP and 4050 ppm K in KIT-SP.

**Table 1.** Summary of stream composition at the different stages of the clean-up process. PNNL-HTL is derived from corn stover, processed using hydrothermal liquefaction (HTL) and originally published elsewhere [13]. USDA-FP is derived from horse litter, processed using fast pyrolysis (FP). KIT-SP is derived from beech wood chips, processed using intermediate screw pyrolysis (SP). More information about the composition can be found in the Supporting Information.

	PNNL-HTL					USDA-FP					KIT-SP				
	Initial	Carbon Treated	Raffinate	Refined Extract	Final Feedstock	Initial	Carbon Treated	Raffinate	Refined Extract	Final Feedstock	Initial	Carbon Treated	Raffinate	Refined Extract	Final Feedstock
%C Retained	100	65.5	26.0	29.0	29.0	100	73.2	15.1	21.7	15.1	100	30.4	11.7	14.9	11.8
%Carboxylic Acid Retained	100	62.6	18.8	34.9	34.9	100	88.9	24.8	53.5	45.9	100	33.5	6.55	22.2	22.4
Acetic Acid [wt.%]	22.3	19.4	7.65	63.4	29.1	4.78	3.07	1.45	39.6	9.24	9.68	6.62	1.80	34.3	20.1
Propionic Acid [wt.%]	3.93	2.33	0.241	11.2	4.79	2.89	1.95	1.47	9.23	1.68	2.72	2.07	1.39	5.42	2.98
Non-Participating Carbon [wt.%]	6.40	6.09	7.89	5.77	0.16	5.95	3.00	5.34	27.33	1.55	13.8	8.03	12.2	41.1	2.57
Total C [wt.%]	32.6	27.8	15.8	80.4	34.0	8.35	8.02	8.26	76.16	12.5	26.2	16.7	15.4	80.8	25.6
S/C <sup>a</sup>					2.8					11.2					4.7
Na [ppm]	7040	7320	8580	25.2	22.9	9.30	202	147	18.3	12.8	28.2	446	365	7.96	9.64
K [ppm]	746	1960	2350	11.6	3.97	12.3	1560	1450	85.2	17.2	15.7	4050	1420	20.5	12.8
S [ppm]	BDL <sup>b</sup>	BDL	BDL	BDL	BDL	10.6	65.1	44.9	BDL	BDL	56.5	68.5	65.8	BDL	BDL

<sup>a</sup> S/C = molar ratio of steam-to-carbon. <sup>b</sup> BDL = below detection limit.

The carbon-treated aqueous phases were then placed inside a continuous LLE to remove and concentrate organic molecules from the aqueous phase. Addition of methyl tert-butyl ether (MTBE) to the carbon-treated aqueous samples created two phases, an aqueous phase (the raffinate) and an organic phase (the extract). Under batch LLE, this process was found to increase the total organic concentration from 34–80 wt %. The continuous LLE used here was found to generate extract (i.e., organic molecules extracted from aqueous phase) with the same concentration as the one obtained in the batch LLE. Further, both LLE systems generated the same amount of extract (e.g.,  $\sim 0.60 \text{ g}_{\text{carboxylic acids}} \text{ g}_{\text{aqueous phase fed}}^{-1}$ ). However, the removal of MTBE was less effective in the continuous LLE than in the rotary-vaporization used in the batch LLE. For example, the extract from the continuous LLE had about 10 times higher concentration of MTBE (20.9 and 35.2 wt % for USDA-FP and KIT-SP respectively) than the extract obtained in batch LLE (2.91 wt % for HTL). Therefore, an additional distillation step was necessary to remove the remaining MTBE from the extract generated in the continuous LLE to produce the final feedstock. The composition of the main constituents found in the streams at the different steps of the clean-up process are summarized in Table 1. A full analysis of the stream can be found in the Supporting Information.

## 2.2. Catalytic Upgrading of Cleaned Up Aqueous Phase to Isobutene

The final PNN-HTL and KIT-SP feedstocks were selected to explore the catalytic upgrading of carboxylic acids into olefins using the  $\text{Zn}_1\text{Zr}_{2.5}\text{O}$  catalyst. The product selectivity and catalyst stability were evaluated as a function of gas hour space velocity (GHSV). The final PNNL-HTL feedstock had a lower concentration of non-participating carbon compared to the final KIT-SP feedstock, 0.16 and 2.57 wt % respectively.

From these GHSV screening (Figure 2), the product distribution obtained with both feedstocks appeared similar to that previously observed with ethanol and propanol [22]. As depicted in Scheme 1 and in our previous work, [22] acetone and iso- and n-butene (i.e., iso- $\text{C}_4$  and n- $\text{C}_4$ ) are direct products of acetic acid. However, methyl ethyl ketone (MEK) and methyl butane ( $\text{C}_5$ ) are produced from the combination of propanoic acid with acetic acid as depicted in Scheme 2. This mechanism also agrees with our recent study for conversion of MEK to olefins over  $\text{Zn}_x\text{Zr}_y\text{O}_z$  catalysts [23]. As shown in Figure 2, the ketone and olefin selectivity are directly affected by the GHSV, emphasizing that the ketones are indeed reaction intermediates for the olefin production as depicted in Schemes 1 and 2. For example, at the highest GHSV (i.e., lowest contact time) there was already complete conversion of the carboxylic acids but we only observed ketone intermediates (e.g., acetone from acetic acid-acetic acid self-ketonization, MEK from acetic acid-propionic acid cross-ketonization, and 3-pentanone from propionic acid self-ketonization). However, the selectivity towards ketone formation decreased as the GHSV decreased (i.e., higher contact time). For example, at  $\sim 1200 \text{ h}^{-1}$  (i.e., the lowest SV studied) there was almost complete conversion of the ketone intermediates to their respective olefins, as illustrated in Schemes 1 and 2, with a combined ketone selectivity of 8.6 and 3.9% for the PNNL-HTL and KIT-SP feedstocks respectively. This suggested that  $\text{Zn}_x\text{Zr}_y\text{O}_z$  is an effective catalyst for the direct production of olefins from carboxylic acids as well as alcohols.

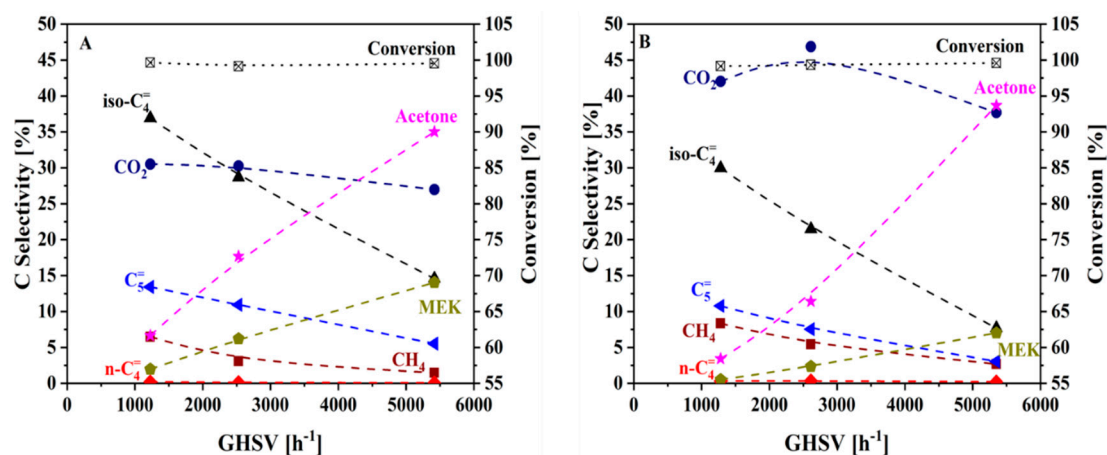
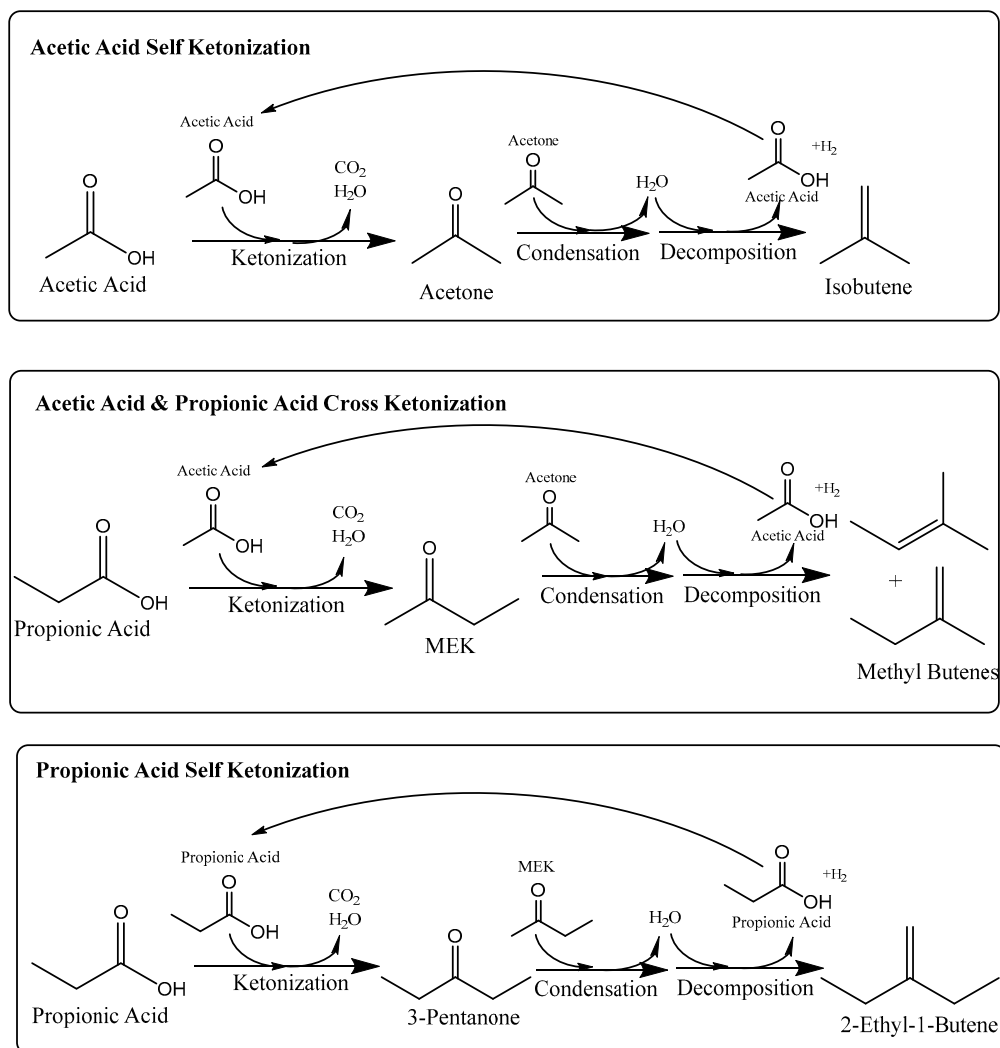


**Figure 2.** Gas hour space velocity (GHSV) profile of (A) PNNL-HTL feedstock, S/C = 2.8, and (B) KIT-SP feedstock, S/C = 4.7. Temperature: 450 °C, catalyst loading 0.7 g, N<sub>2</sub> 50 vol%. Complete conversion of carboxylic acids was observed at all GHSV's studied. 3-pentanone was observed in trace (0.21% for PNNL-HTL and 0.10% for KIT-SP) amounts at ~5400 h<sup>-1</sup>, but was otherwise not observed.



**Scheme 2.** Reaction network of carboxylic acid to olefin ethanol to isobutene and major side products.

As shown in Figure 3, the overall product selectivity obtained with the three feedstocks favors olefin over ketone formation when operated at low GHSV and same reaction conditions, however, the individual olefin selectivity differs. For example, the PNNL-HTL and HIT-SP feedstocks were ~15% selective towards  $C_5^+$  production, the USDA-FP sample was  $\geq 5\%$ . We hypothesize this difference in  $C_5^+$  selectivity is due to the differences in acetic acid and propanoic acid concentration. For example, PNNL-HTL feedstocks had the highest overall concentration of carboxylic acids (33.9 wt %) and propanoic acid (4.79 wt %), while the USDA-FP feedstock had the lowest overall concentration of carboxylic concentration (10.9 wt %) and propanoic acid (1.68 wt %).

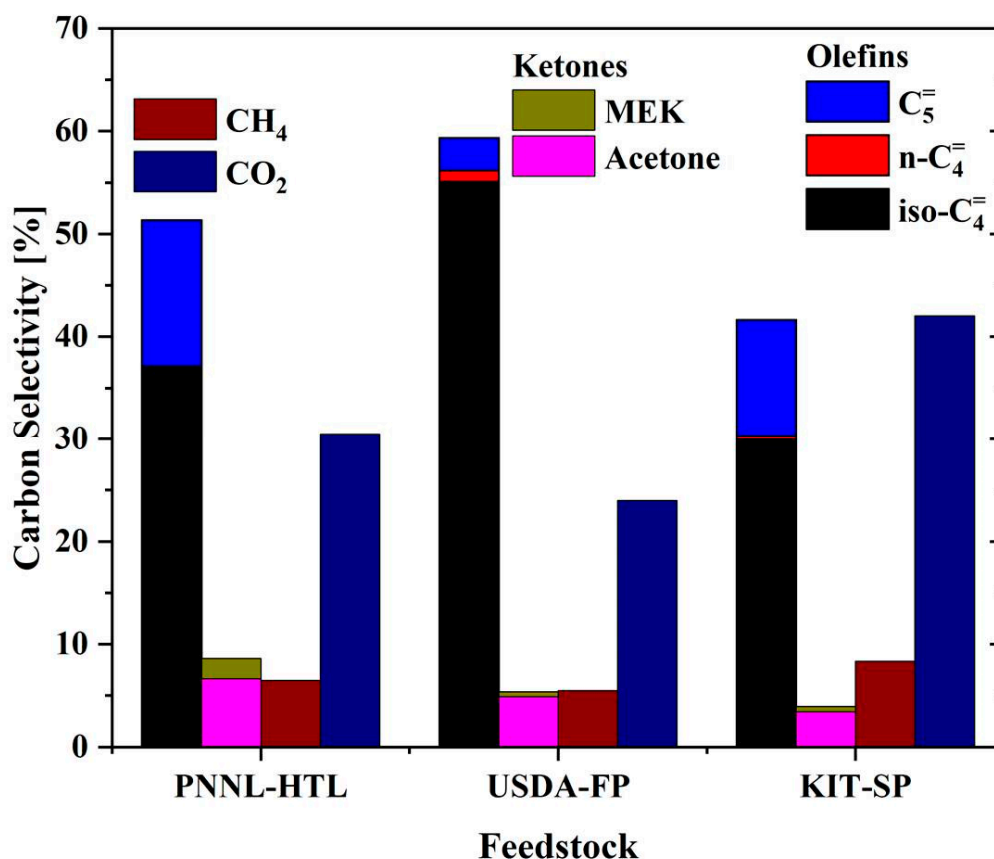


**Figure 3.** Major product selectivity of all feedstocks. Temperature: 450 °C, GHSV: 1200 h<sup>-1</sup>, catalyst loading 0.7 g, N<sub>2</sub> 50 vol%, S/C = 2.8, 11.2, 4.7 for PNNL-HTL, USDA-FP, and KIT-SP, respectively. The product selectivity was measured at 100% conversion of carboxylic acids.

Figure 4 depicts the stability of the Zn<sub>1</sub>Zr<sub>2.5</sub>O catalyst when tested with the PNNL-HTL and KIT-SP feedstocks containing different concentrations of non-participating carbon species, 0.16 and 2.57 wt %, respectively. The initial and final conversion and primary product selectivities are summarized in Table 2. The PNNL-HTL feedstock (with the lowest non-participating carbon concentrations) showed a stability profile like the one previously observed with model ethanol feedstocks [19,22]. While the higher GHSV did increase selectivity to the ketone products (~23.5 and ~10.0% for acetone and MEK respectively) overall selectivity was relatively stable for ~20 h time on stream (TOS), after which the ketone selectivity began increasing significantly while olefin selectivity decreased. This further supported our speculation that the ketones are the intermediate of the olefins. In contrast, the KIT-SP feedstock started with higher ketone selectivity, ~49% selectivity at 10 h TOS, and continued to increase for the duration of the test, ~65% selectivity by 22 h TOS. While the conversion was constant with the PNNL-HTL feedstock at 100% for the duration of the experiment, it decreased with the KIT-SP feedstock. As shown in Figure 4B, the conversion started to decrease at 26 h TOS and dropped to 82% by the end of the experiment. This difference in stability with the two feedstocks indicated that, while

the  $Zn_xZr_yO_z$  catalyst can accommodate a range of compounds, the catalyst will deactivate faster in the presence of more non-participating compounds in the feedstock [13].

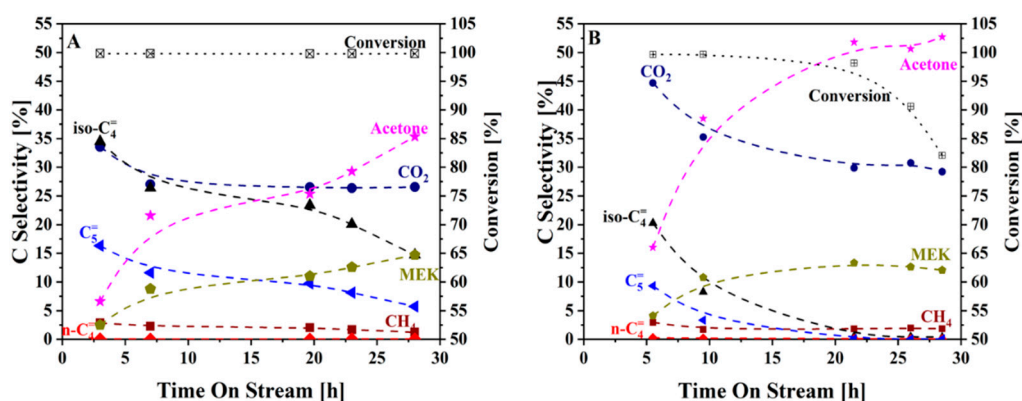


**Figure 4.** High GHSV stability of (A) PNNL-HTL feedstock, S/C = 2.8, and (B) KIT-SP feedstock, S/C = 4.7. Temperature: 450 °C, GHSV: 5500 h<sup>−1</sup>, catalyst loading 0.7 g, N<sub>2</sub> 50 vol%.

**Table 2.** Comparison of initial and final activity and selectivity of PNNL-HTL and KIT-SP feedstocks shown in Figure 4.

	PNNL-HTL		KIT-SP	
	Initial	Final	Initial	Final
Conversion (%)	99.8	99.8	99.7	82.1
Selectivity (%)				
All Olefins	53.2	21.5	30.8	0.77
All Ketones	9.11	50.0	20.1	64.8
Isobutene	34.5	14.7	20.2	0.39
Acetone	6.60	35.3	16.0	52.7

The long-term stability of the  $Zn_xZr_yO_z$  catalyst (Figure 5) was tested with the USDA-FP feedstock as it had the lowest total carboxylic acid content and some non-participating carbon compounds, 10.9 and 1.55 wt %, respectively. We chose a low SV (1200 h<sup>−1</sup>) to maximize olefin production which is more representative of industrial targets. The  $Zn_xZr_yO_z$  catalyst was relatively stable for close to 100 h, and by 95 h TOS the isobutene selectivity was stable >50% (net olefins ~60%). The ketone selectivity, particularly acetone, slowly increased over this period from 3.4% at 47 h TOS to 8.9% at 95 h TOS. At 120 h TOS the  $Zn_xZr_yO_z$  catalyst showed catalytic deactivation as ketone breakthrough was observed, with ketone selectivity at 25.3% (23.9% and 1.37% for acetone and MEK respectively). Following in situ catalyst regeneration, the  $Zn_xZr_yO_z$  showed complete recovery of activity with isobutene selectivity increasing to 58.5% and acetone selectivity dropping back to 2.70%. The catalysts showed catalyst deactivation after another 50 h of reaction as acetone selectivity increased to 7.49%. A second in situ catalyst regeneration completely regenerated the  $Zn_xZr_yO_z$  activity.

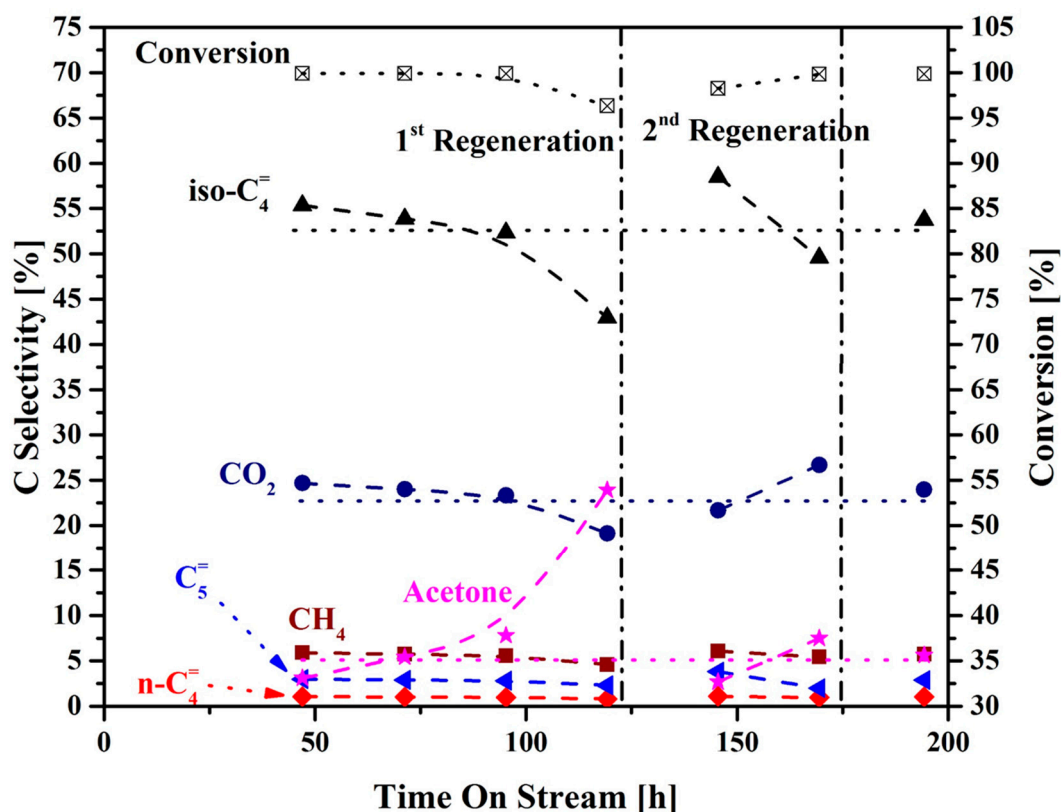


**Figure 5.** Stability and regeneration of USDA-FP feedstock. Temperature: 450 °C, S/C = 11.2, GHSV: 1200 h<sup>−1</sup>, catalyst loading 0.7 g, N<sub>2</sub> 50 vol%. The catalyst regeneration was done by calcination in 5 vol% O<sub>2</sub> in N<sub>2</sub> at 500 °C for 4 h.

### 2.3. Catalytic Upgrading of Ethanol to Propene

H<sub>2</sub> is often used to improve catalyst stability, however the role of H<sub>2</sub> on the olefin formation reactions has not been widely studied [1,12,22]. Whereas H<sub>2</sub> could hydrogenate olefins into paraffins, it could also hydrogenate reaction intermediates and shift the product distribution towards different olefin products. As shown in Scheme 1, acetone can be hydrogenated to isopropanol which then can dehydrate to propene. To simplify this portion of our study, a 20 wt % ethanol in water feed was used rather than the more complex aqueous phase feedstocks discussed earlier. Propene production in the absence of H<sub>2</sub> from the complex feedstocks (i.e., PNHL-HTL, USDA-FP, and KIT-SP) was negligible (<1% selectivity, typically ~0.2% selectivity).

As shown in Figure 6, the propene selectivity was enhanced by cofeeding H<sub>2</sub>. For example, when the N<sub>2</sub> carrier gas was replaced by H<sub>2</sub> in 25 vol% increments, the propene (C<sub>3</sub>H<sub>6</sub>) selectivity increased roughly linearly with H<sub>2</sub> composition from 5.40 to 18.6%, while the isobutene selectivity decreased from 43.1 to 32.6%. The change in product distribution is because the hydrogenation of acetone (and subsequent dehydration to produce propene) is enhanced in the presence of H<sub>2</sub> while acetone self-condensation (to produce isobutene) is inhibited as depicted in Scheme 1 and described in our previous work [22]. Further, the CO<sub>2</sub> selectivity also decreased as a result of inhibiting the isobutene formation as expected from the reaction network described in Scheme 1. The CH<sub>4</sub> selectivity remained relatively constant at ~4%, indicating that changing the gas environment does not significantly impact decomposition or methanation reactions. We speculate that cofeeding H<sub>2</sub> during the upgrading of the feedstocks explored in this work over the Zn<sub>x</sub>Zr<sub>y</sub>O<sub>z</sub> would cause a similar enhancement in propene production and shift the C<sub>5</sub>= production more towards C<sub>4</sub>= [23]. The mixed olefin product stream could be then oligomerized to higher value products as demonstrated by Saavedra Lopez et al. [14].

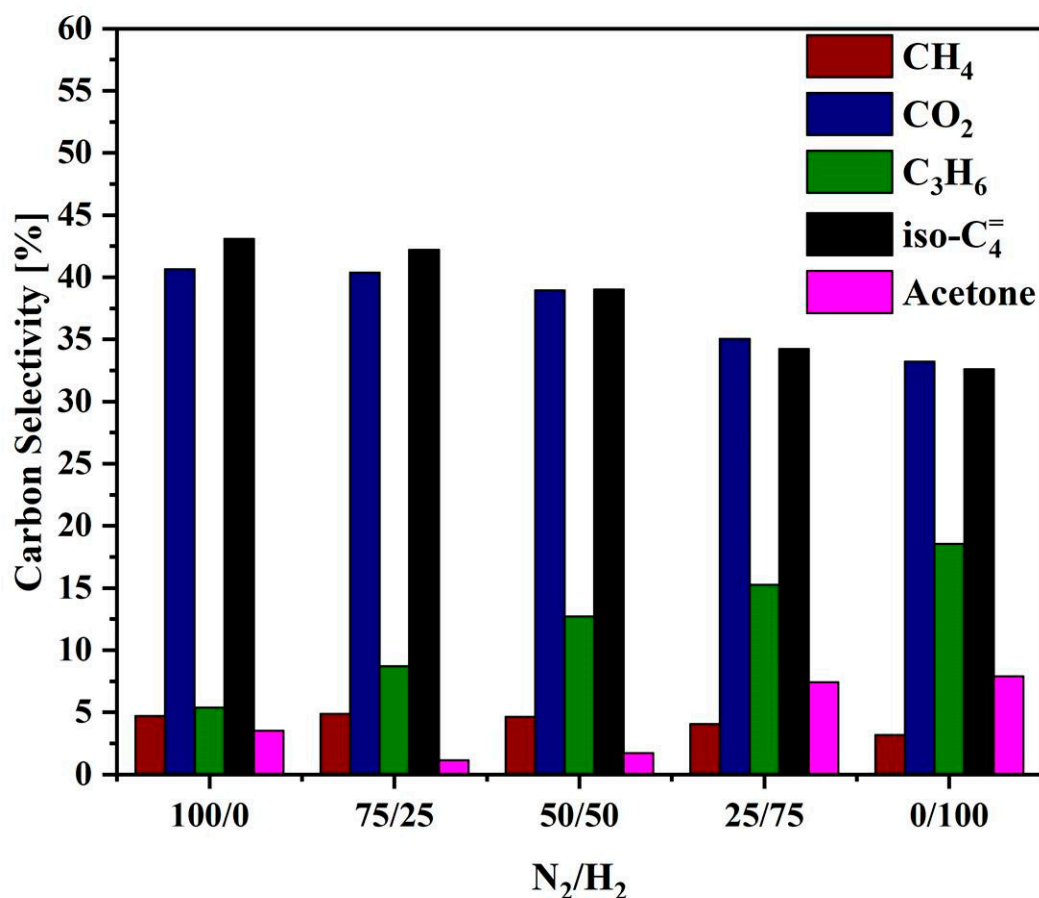


**Figure 6.** Effect of gas environment on product selectivity. Feedstock: 20 wt % ethanol in water, S/C = 5.1, Temperature: 450 °C, GHSV: 1200 h<sup>−1</sup>, catalyst loading 0.7 g, N<sub>2</sub>/H<sub>2</sub> composition was constant at 50 vol%.

### 3. Materials and Methods

#### 3.1. Feedstock Sources

Three different feedstocks were investigated during this study. The first feedstock, provided by PNNL and designated PNNL-HLT, was the same as used in a prior study [13]. Briefly, the aqueous feed produced from HTL of corn stover was used and modified to simulate ~100 recycles in the HTL system to reach the desired concentration of organic compounds in the aqueous phase [4,13,25]. The second feedstock, provided by USDA and designated USDA-FP, was produced using FP of horse litter. Details on the FP system can be found elsewhere; briefly, the horse litter was fed via hopper to a novel FP system where a fluidized bed is used to perform the fast pyrolysis, recycled process gas can also be used to decrease the oxygen content of the final oil, the effluent from the fluidized bed is then passed through a cyclone separator for solid removal, and a condenser train was used for sample collection [11,26,27]. The third feedstock, provided by KIT and designated KIT-SP, was produced using STYX screw pyrolysis of bark-free beech wood pellets. Details on the STYX screw pyrolysis system can be found elsewhere; briefly, the wood pellets were fed via hopper to an integrated pyrolysis reactor with a screw mechanism to drive material through the reactor, product gasses are removed at various points along the integrated reactor and sent to a condenser train for sample collection, filters in the reactor prevent solids from being entrained in the gas flows, and all solids are removed at the end to the of the reactor at the screw outlet [10,28,29].

### 3.2. Feedstock Clean Up

A multi-step process was used to clean up the various bio-oil aqueous phases shown in Figure 7. The PNNL-HTL feedstock is the same as reported previously, cleaned using the batch process first reported [13]. The USDA-FP and KIT-SP feedstocks were both cleaned using continuous liquid–liquid extraction. First the as received feedstocks were treated with activated carbon (AC) obtained from Pacific Activated Carbon Co. Inc. (PACCO, CTC, coconut shell, lot# 2007-2-22AC) to remove trace contaminants from the blended HTL-derived aqueous feed at an AC/feedstock ratio of  $1/10$  by weight. The slurry was capped to avoid evaporation of  $H_2O$  and light organics and agitated at 250 rpm at ambient temperature for 24 h. The AC was then removed via vacuum filtration. For USDA-FP, two carbon treatments were sufficient to achieve the desired color change of the feedstock. For KIT-SP, five carbon treatments were required to achieve the desired color change of the feedstock (Supporting Figure S1). Methyl tert-butyl ether (MTBE; Sigma-Aldrich, anhydrous 99.8%) was then used as a solvent to extract the desired carboxylic acid molecules (acetic acid and propanoic acid) from the carbon-treated mixture at a mixture/MTBE ratio of  $\sim 1/1$  by weight. The carbon-treated mixture and the MTBE were charged into a continuous liquid–liquid extraction vessel (Figure 1) and MTBE circulated internally for  $\sim 48$  h. After separation, the MTBE and raffinate from the extractor were placed in a cone-shaped separatory funnel to separate the MTBE (top) and the raffinate (bottom) ( $\sim 10$  min). The MTBE was combined with the collection pot to form the extract. The extract was then boiled to remove the majority of MTBE. This MTBE was then recycled for subsequent extractions. The refined extract, containing mostly acetic acid, propanoic acid, and residual MTBE was diluted with deionized (DI) water to have enough material for benchtop distillation. The distillation resulted in two cuts and the pot residual. The first cut was the majority of the residual MTBE, while the second cut had the lightest components from the refined extract. The final feedstock was made by combining the second cut from distillation, the pot residual, and DI  $H_2O$  to adjust the acetic acid concentration to the desired amount. For easy comparison of the concentration of organics across feedstocks, the molar ratio of steam-to-carbon (S/C) was used, that is, the molar ratio of water to the total number of moles of carbon in the feedstock. Non-participating carbon refers to any compound detected via LC that does not appear in the reaction network shown in Scheme 1, that is, non-alcohol, non-ketone, and non-carboxylic acid compounds.

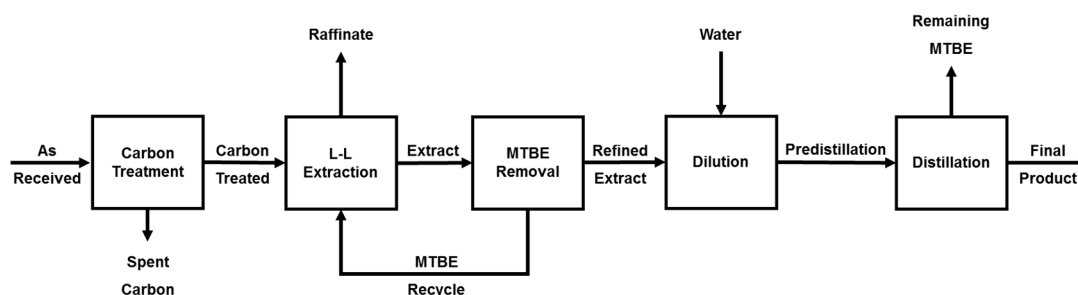


Figure 7. Clean up protocol for bio-oil aqueous phase prior to testing adapted from Davidson et al. [13].

### 3.3. Catalyst Preparation

Mixed oxide catalysts were synthesized via wet impregnation of a  $\text{Zn}(\text{NO}_3)_2 \cdot 6\text{H}_2\text{O}$  solution on  $\text{Zr}(\text{OH})_4$  as described elsewhere [22]. The  $\text{Zr}(\text{OH})_4$  was initially dried overnight at 105 °C to remove any excess water on the surface before impregnation. After impregnation, the catalysts were dried overnight at room temperature and then for 4 h at 105 °C prior to calcination. The catalysts then were calcined via a 3 °C min<sup>−1</sup> ramp to 400 °C for 2 h, followed by a 5 °C min<sup>−1</sup> ramp to the final calcination temperature of 550 °C for 3 h. Extensive details of the catalyst characteristics have been published previously and are not reproduced here [19–22].

### 3.4. Reactor and Reaction Conditions

Olefin production reactions were performed in a  $\frac{1}{2}$ " inch outer-diameter, fixed-bed alumina reactor. Alumina reactors were used to minimize potential side reactions that might occur with stainless steel reactors. Typically, 0.70 g of  $\text{Zn}_x\text{Zr}_{1-x}\text{O}_2$  was loaded undiluted. Prior to testing, catalysts were degassed under  $\text{N}_2$  at 450 °C for 8 h.

The catalysts were tested at atmospheric pressure and at a reaction temperature of 450 °C. The liquid feed was fed via HPLC pump to a vaporizer held at 150 °C. A  $\text{N}_2$  gas flow rate (typically ~50 mol% in the feed) was introduced into the system to serve as the carrier gas and internal reference standard. Both liquid and gas feed were adjusted accordingly to achieve desired GHSV. On-line gas products were tracked via four-channel MicroGC<sup>®</sup> and condensable products were analyzed off line via LC analysis, as described previously [13]. The reported conversion is based on the ratio of feed carboxylic acids to carboxylic acids remaining after reaction. For all reactions total carbon balance was >95% and measurement errors in composition are <1%.

## 4. Conclusions

In this study we demonstrated a cleanup process, previously reported using batch processing, here adapted to continuous flow liquid–liquid extraction. Aqueous phases, rich in carboxylic acids, were obtained from several liquefaction processes, including HTL, FP, and SP, and evaluated for cleanup and catalytic upgrading. Future advances to the cleanup process are required in order to improve hydrocarbon retention. Cleaned feedstocks were converted to primarily  $\text{C}_4$  and  $\text{C}_5$  olefins, and  $\text{CO}_2$  over a  $\text{Zn}_x\text{Zr}_y\text{O}_z$  mixed oxide catalyst. The reaction network appears consistent with previous reports using model ethanol and acetic acid feedstocks. Carboxylic acids are converted primarily to iso-olefins over  $\text{Zn}_x\text{Zr}_y\text{O}_z$  catalyst. Specifically, iso-butene is produced from acetic acid, a primary constituent from the biomass-derived aqueous phase. Conversion of acetic acid and propionic acid over  $\text{Zn}_x\text{Zr}_y\text{O}_z$  involve cross-coupling reactions and produce branched  $\text{C}_5$  olefins. Non-participating hydrocarbons in the feedstock (e.g., sugars, polyols) are not believed to participate in the reaction mechanism through ketone intermediates and contribute to catalyst deactivation. Finally, the presence of  $\text{H}_2$  in the feed was found to facilitate hydrogenation of intermediate acetone, thereby increasing propene production and, consequently, decreasing isobutene production.

**Supplementary Materials:** The following are available online at <http://www.mdpi.com/2073-4344/9/11/923/s1>, Table S1: LC analysis of USDA-FP feedstock after key steps of clean up protocol, Table S2: LC analysis of KIT-SP feedstock after key steps of clean up protocol, Table S3: ICP analysis of USDA-FP feedstock after key steps of clean up protocol, Table S4: ICP analysis of KIT-SP feedstock after key steps of clean up protocol, Figure S1: KIT-SP feedstock A) Initial B) During Carbon Treatment, After Third Carbon Treatment ~72 h C) After All Carbon Treatment, Five Carbon Treatments ~120 h, Table S5: Summary of dilute feedstock cleanup.

**Author Contributions:** S.D.D. lead most experiments, data analysis, and operations. J.A.L.-R. contributed to the development of the cleanup protocol. M.F. synthesized and prepared the  $\text{Zn}_x\text{Zr}_y\text{O}_z$  catalyst. A.R.C., Y.E., and M.T.M. provided the major feedstocks studied in this work (PNNL-HTL, USDA-FP, and KIT-SP respectively). V.L.D., K.O.A., and R.A.D. lead conceptualization, project administration, and funding acquisition.

**Funding:** This work was financially supported by the U.S. Department of Energy's (DOE) Bioenergy Technologies Office under Contract DE-AC05-76RL01830 and in collaboration with the Chemical Catalysis for Bioenergy Consortium (ChemCatBio), a member of the Energy Materials Network (EMN), and was performed at Pacific Northwest National Laboratory (PNNL). PNNL is a multi-program national laboratory operated for the DOE by Battelle Memorial Institute.

**Acknowledgments:** The authors thank Teresa Lemmon for analytical support of this work and collaborators at NREL for providing dilute feedstocks. ARS acknowledges the help of Mark Schaffer and Neil Goldberg for operation of the pyrolysis system. The views and opinions of the authors expressed herein do not necessarily state or reflect those of the United States Government or any agency thereof. Neither the United States Government nor any agency thereof, nor any of their employees, makes any warranty, expressed or implied, or assumes any legal liability or responsibility for the accuracy, completeness, or usefulness of any information, apparatus, product, or process disclosed, or represents that its use would not infringe privately owned rights.

**Conflicts of Interest:** The authors declare no conflict of interest. The funders had no role in the design of the study; in the collection, analyses, or interpretation of data; in the writing of the manuscript; or in the decision to publish the results.

## Abbreviations

AC	Activated carbon
BDL	Below detection limit
DI	Deionized
FP	Fast pyrolysis
GHSV	Gas hourly space velocity
HTL	Hydrothermal liquefaction
KIT	Karlsruhe Institute of Technology
LLE	Liquid–liquid extraction
MEK	Methyl ethyl ketone (butanone)
MTBE	Methyl Tert-butyl ether
PNNL	Pacific Northwest National Lab
S/C	Steam-to-carbon ratio (molar ratio)
SP	Screw pyrolysis
SV	Space velocity
TOS	Time on stream
USDA	United States Department of Agriculture

## Appendix A

Operating conditions of the LLE proved critical to optimizing organic extraction. For these extractions the heavy solvent valve was closed. Carbon-treated feed was first charged into the extraction column. Then the remaining height of the extraction column was filled with MTBE. To control the ratio of solvent to feedstock, the remaining quantity of MTBE was then charged into the collection flask. Once charged, the glass fittings were all sealed with vacuum grease and clamps. The circulator for the condenser was set to 5 °C and allowed to equilibrate before starting heating. A stir bar and plate with no heating provided mixing to the extraction column, while a stir bar and plate with heating via mineral oil bath provided heat and mixing to the collection flask. A low flow of N<sub>2</sub> was applied to the head space above the condenser to minimize loss of material during extraction. Once equilibrated at ambient temperature the mineral oil bath was heated to 80 °C; this vaporized the MTBE from the collection flask to the condenser, where it condensed and ran down a drip tube to the bottom of the extraction flask. As the MTBE rose through the extraction flask it extracted the target organics from the feedstock. Upon reaching the top of the extraction flask, the organic rich MTBE then flowed back to the collection flask where the MTBE vaporized again but the other organics did not. This stable cycle of the LLE was then continued for ~48 h.

## References

1. Huber, G.W.; Iborra, S.; Corma, A. Synthesis of Transportation Fuels from Biomass: Chemistry, Catalysts, and Engineering. *Chem. Rev.* **2006**, *106*, 4044–4098. [[CrossRef](#)] [[PubMed](#)]
2. Bond, J.Q.; Upadhye, A.A.; Olcay, H.; Tompsett, G.A.; Jae, J.; Xing, R.; Alonso, D.M.; Wang, D.; Zhang, T.; Kumar, R.; et al. Production of renewable jet fuel range alkanes and commodity chemicals from integrated catalytic processing of biomass. *Energy Environ. Sci.* **2014**, *7*, 1500–1523. [[CrossRef](#)]
3. Huber, G.W.; Corma, A. Synergies between Bio- and Oil Refineries for the Production of Fuels from Biomass. *Angew. Chem. Int. Ed.* **2007**, *46*, 7184–7201. [[CrossRef](#)] [[PubMed](#)]

4. Zhu, Y.; Biddy, M.J.; Jones, S.B.; Elliott, D.C.; Schmidt, A.J. Techno-economic analysis of liquid fuel production from woody biomass via hydrothermal liquefaction (HTL) and upgrading. *Appl. Energy* **2014**, *129*, 384–394. [[CrossRef](#)]
5. Chheda, J.N.; Huber, G.W.; Dumesic, J.A. Liquid-phase catalytic processing of biomass-derived oxygenated hydrocarbons to fuels and chemicals. *Angew. Chem. Int. Ed.* **2007**, *46*, 7164–7183. [[CrossRef](#)] [[PubMed](#)]
6. Panisko, E.; Wietsma, T.; Lemmon, T.; Albrecht, K.; Howe, D. Characterization of the aqueous fractions from hydrotreatment and hydrothermal liquefaction of lignocellulosic feedstocks. *Biomass Bioenergy* **2015**, *74*, 162–171. [[CrossRef](#)]
7. Zhang, Q.; Chang, J.; Wang, T.; Xu, Y. Review of biomass pyrolysis oil properties and upgrading research. *Energy Convers. Manag.* **2007**, *48*, 87–92. [[CrossRef](#)]
8. Elliott, D.C.; Beckman, D.; Bridgwater, A.V.; Diebold, J.P.; Gevert, S.B.; Solantausta, Y. Developments in direct thermochemical liquefaction of biomass: 1983–1990. *Energy Fuels* **1991**, *5*, 399–410. [[CrossRef](#)]
9. Elliott, D.C.; Biller, P.; Ross, A.B.; Schmidt, A.J.; Jones, S.B. Hydrothermal liquefaction of biomass: Developments from batch to continuous process. *Bioresour. Technol.* **2015**, *178*, 147–156. [[CrossRef](#)]
10. Funke, A.; Tomasi Morgano, M.; Dahmen, N.; Leibold, H. Experimental comparison of two bench scale units for fast and intermediate pyrolysis. *J. Anal. Appl. Pyrolysis* **2017**, *124*, 504–514. [[CrossRef](#)]
11. Boateng, A.A.; Daugaard, D.E.; Goldberg, N.M.; Hicks, K.B. Bench-Scale Fluidized-Bed Pyrolysis of Switchgrass for Bio-Oil Production. *Ind. Eng. Chem. Res.* **2007**, *46*, 1891–1897. [[CrossRef](#)]
12. Huber, G.W.; Dumesic, J.A. An overview of aqueous-phase catalytic processes for production of hydrogen and alkanes in a biorefinery. *Catal. Today* **2006**, *111*, 119–132. [[CrossRef](#)]
13. Davidson, S.D.; Lopez-Ruiz, J.A.; Zhu, Y.; Cooper, A.R.; Albrecht, K.O.; Dagle, R.A. Clean up and Catalytic Upgrading of Hydrothermal Liquefaction-Derived Aqueous Phase into Fuels and Chemicals via Ketone Intermediates. *ACS Sustain. Chem. Eng.* **2019**. submitted.
14. Saavedra, L.J.; Dagle, R.A.; Dagle, V.L.; Smith, C.; Albrecht, K.O. Oligomerization of ethanol-derived propene and isobutene mixtures to transportation fuels: Catalyst and process considerations. *Catal. Sci. Technol.* **2019**, *9*, 1117–1131. [[CrossRef](#)]
15. Dagle, V.L.; Smith, C.; Flake, M.; Albrecht, K.O.; Gray, M.J.; Ramasamy, K.K.; Dagle, R.A. Integrated process for the catalytic conversion of biomass-derived syngas into transportation fuels. *Green Chem.* **2016**, *18*, 1880–1891. [[CrossRef](#)]
16. Yoon, J.W.; Chang, J.-S.; Lee, H.-D.; Kim, T.-J.; Jhung, S.H. Trimerization of isobutene over a zeolite beta catalyst. *J. Catal.* **2007**, *245*, 253–256. [[CrossRef](#)]
17. Marchionna, M.; Di Girolamo, M.; Patrini, R. Light olefins dimerization to high quality gasoline components. *Catal. Today* **2001**, *65*, 397–403. [[CrossRef](#)]
18. Carr, A.G.; Dawson, D.M.; Bochmann, M. Zirconocenes as Initiators for Carbocationic Isobutene Homo- and Copolymerizations. *Macromolecules* **1998**, *31*, 2035–2040. [[CrossRef](#)]
19. Liu, C.; Sun, J.; Smith, C.; Wang, Y. A study of Zn<sub>x</sub>Zr<sub>y</sub>O<sub>z</sub> mixed oxides for direct conversion of ethanol to isobutene. *Appl. Catal. A Gen.* **2013**, *467*, 91–97. [[CrossRef](#)]
20. Sun, J.; Baylon, R.A.L.; Liu, C.; Mei, D.; Martin, K.J.; Venkatasubramanian, P.; Wang, Y. Key Roles of Lewis Acid–Base Pairs on Zn<sub>x</sub>Zr<sub>y</sub>O<sub>z</sub> in Direct Ethanol/Acetone to Isobutene Conversion. *J. Am. Chem. Soc.* **2015**, *138*, 507–517. [[CrossRef](#)]
21. Sun, J.; Zhu, K.; Gao, F.; Wang, C.; Liu, J.; Peden, C.H.F.; Wang, Y. Direct Conversion of Bio-ethanol to Isobutene on Nanosized Zn<sub>x</sub>Zr<sub>y</sub>O<sub>z</sub> Mixed Oxides with Balanced Acid–Base Sites. *J. Am. Chem. Soc.* **2011**, *133*, 11096–11099. [[CrossRef](#)] [[PubMed](#)]
22. Smith, C.; Dagle, V.; Flake, M.; Ramasamy, K.; Kovarik, L.; Bowden, M.; Onfroy, T.; Dagle, R. Conversion of Syngas-Derived C<sub>2</sub>+ Mixed Oxygenates to C<sub>3</sub>–C<sub>5</sub> Olefins over Zn<sub>x</sub>Zr<sub>y</sub>O<sub>z</sub> Mixed Oxides Catalysts. *Catal. Sci. Technol.* **2016**, *6*, 2325–2336. [[CrossRef](#)]
23. Dagle, V.L.; Dagle, R.A.; Kovarik, L.; Baddour, F.; Habas, S.E.; Elander, R. Single-step Conversion of Methyl Ethyl Ketone to Olefins over Zn<sub>x</sub>Zr<sub>y</sub>O<sub>z</sub> Catalysts in Water. *ChemCatChem* **2019**, *11*, 3393–3400. [[CrossRef](#)]
24. Crisci, A.J.; Dou, H.; Prasomsri, T.; Román-Leshkov, Y. Cascade Reactions for the Continuous and Selective Production of Isobutene from Bioderived Acetic Acid Over Zinc-Zirconia Catalysts. *ACS Catal.* **2014**, *4*, 4196–4200. [[CrossRef](#)]

25. Schmidt, A.J.; Lindstorm, T.; Talmadge, M.; Zhu, Y. Mid Stage 2 Report on Hydrothermal Liquefaction Strategy for the NABC Leadership Team. In *PNNL-21768*; Energy, U.S.D.O., Ed.; Pacific Northwest National Laboratory: Richland, WA, USA, 2012.
26. Mullen, C.A.; Boateng, A.A.; Goldberg, N.M. Production of Deoxygenated Biomass Fast Pyrolysis Oils via Product Gas Recycling. *Energy Fuels* **2013**, *27*, 3867–3874. [[CrossRef](#)]
27. Boateng, A.A.; Schaffer, M.A.; Mullen, C.A.; Goldberg, N.M. Mobile demonstration unit for fast- and catalytic pyrolysis: The combustion reduction integrated pyrolysis system (CRIPS). *J. Anal. Appl. Pyrolysis* **2019**, *137*, 185–194. [[CrossRef](#)]
28. Tomasi Morgano, M.; Leibold, H.; Richter, F.; Seifert, H. Screw pyrolysis with integrated sequential hot gas filtration. *J. Anal. Appl. Pyrolysis* **2015**, *113*, 216–224. [[CrossRef](#)]
29. Tomasi Morgano, M.; Leibold, H.; Richter, F.; Stapf, D.; Seifert, H. Screw pyrolysis technology for sewage sludge treatment. *Waste Manag.* **2018**, *73*, 487–495. [[CrossRef](#)] [[PubMed](#)]



© 2019 by the authors. Licensee MDPI, Basel, Switzerland. This article is an open access article distributed under the terms and conditions of the Creative Commons Attribution (CC BY) license (<http://creativecommons.org/licenses/by/4.0/>).